ELSEVIER

Journal of Organometallic Chemistry 573 (1999) 313–322

Journal of Organometallic Chemistry

Syntheses and structural characterisation of the compounds $[Pd(dba)L_2]$ (where $L = PBz_3$ and PPh_2Np) and the novel dimer $[Pd_2(\mu\text{-dba})(\mu\text{-}SO_2)(PBz_3)_2]$[1]

Andrew D. Burrows [b], Nick Choi [c], Mary McPartlin [c], D. Michael P. Mingos [a,*],
Stephen V. Tarlton [a], Ramón Vilar [a]

[a] *Department of Chemistry, Imperial College of Science, Technology and Medicine, South Kensington, London SW7 2AY, UK*
[b] *Department of Chemistry, University of Bath, Claverton Down, Bath BA2 7AY, UK*
[c] *School of Applied Chemistry, University of North London, London N7 8DB, UK*

Received 10 June 1998; accepted 5 July 1998

Abstract

In this paper we report the synthesis and structural characterisation (when $L = PBz_3$ and PPh_2Np) of the compounds $[Pd(dba)L_2]$ (where L, PPh_2Np **1**, PPh_2An **2**, $PPhNp_2$ **3** and PBz_3 **4**; Np, 1-naphthyl; An, anthracenyl; Bz, benzyl; and dba, dibenzylideneacetone) from $[Pd_2(dba)_3]$ and the corresponding phosphine. All these complexes with the exception of **4** retain their structures in solution. The ^{31}P-NMR spectrum of **4** is both solvent and temperature dependent. Under an SO_2 atmosphere the reaction between $[Pd_2(dba)_3]$ and PBz_3 gave the novel dimer $[Pd_2(\mu\text{-dba})(\mu\text{-}SO_2)(PBz_3)_2]$, **5**, which has been structurally characterised. In this dimer both the dba and SO_2 ligands bridge the two metal centres. © 1999 Elsevier Science S.A. All rights reserved.

Keywords: Palladium; Dibenzylideneacetone; Phosphine complexes; Sulphur dioxide complexes

1. Introduction

Palladium complexes of dibenzylideneacetone (dba) [1] have been extensively used as reagents for many organometallic syntheses [2]. They are stable in air and easy to prepare but remain sufficiently labile to function as convenient sources of palladium(0) fragments. With palladium, the following complexes have been prepared and characterised: $[Pd(dba)_2]$, $[Pd(dba)_3]$ and $[Pd_2(dba)_3]$·Solvent [3]. The substitution of dba by phosphines is an important synthetic route to palladium(0)–phosphine complexes. However, the products obtained are not always the simple $[PdL_n]$ complexes as was initially thought. The reaction products seem to be highly dependent on the steric and electronic properties of the phosphine. For example, Ibers and his co-workers showed that $[Pd(dba)_2]$ and $[Pd_2(dba)_3]$ reacted with an excess of triphenylphosphine to give $[Pd(PPh_3)_4]$ [1]. More recent studies have shown that the reaction is more complex and a number of species are present in Ref. [4]. On the other hand, Herrmann and his co-workers have shown that on reacting two equivalents of a phosphine with $[Pd(dba)_2]$, it is possible to isolate complexes in which both the phosphine and the dba are retained [5]. They reported the only structurally characterised example of this type of complex, i.e. $[Pd(dba)(dppe)_2]$ (where $dppe = Ph_2P(CH_2)_2PPh_2$), and ^{31}P-NMR studies of analogous compounds with other phosphines. Similar results have been obtained by Braunstein and co-workers when using phosphines containing a keto or amido function (e.g. $Ph_2PCH_2C(O)Ph$

---

* Corresponding author. Fax: +44 171 5945804; e-mail: d.mingos@ic.ac.uk

[1] Dedicated to Professor Brian Johnson on the occasion of his 60th birthday.

PII S0022-328X(98)00877-8

and $Ph_2PCH_2C(O)NPh_2$) [6]. More recently, Hartwig has reported the formation of the complexes $[PdL_2]$ (L = P(*o*-Tol)$_3$, $P\{2,4\text{-}(Me)_2C_6H_3\}_3$, $P(2\text{-}Me\text{-}4\text{-}FC_6H_3)_3$, PBu^t_3) when reacting $[Pd(dba)_2]$ with the corresponding phosphine [7]. Presumably, the steric bulk of the phosphines is inconsistent with the simultaneous coordination of the dba molecule and results in the formation of the homoleptic phosphine complexes.

$[Pd_2(dba)_3]{\cdot}CHCl_3$ has also been used extensively as starting material for the synthesis of palladium cluster compounds [8,9]. The reactions between $[Pd_2(dba)_3]{\cdot}CHCl_3$ and tertiary phosphines in the presence of small molecules such as CO or SO_2 give rise to cluster compounds whose nuclearity and geometry generally depend on the electronic and steric properties of the phosphine.

In this paper we report the syntheses and characterisation of $[Pd(dba)L_2]$ (where L = PPh_2Np, PPh_2An, $PPhNp_2$, PBz_3) from $[Pd_2(dba)_3]$ and the corresponding phosphine. The products in which the phosphines are PPh_2Np and PBz_3 have been structurally characterised. When the reaction with PBz_3 was carried out in an SO_2 atmosphere, the novel dimer $[Pd_2(\mu\text{-dba})(\mu\text{-}SO_2)(PBz_3)_2]$ was isolated and structurally characterised.

2. Results and discussion

2.1. Reaction of $[Pd_2(dba)_3]$ with bulky aromatic phosphines

The coordination of polyaromatic phosphines to gold(I) and platinum(II) has been recently studied in these laboratories [10,11]. By altering the number of aromatic rings in closely related phosphines, it is possible to fine-tune the electronic and steric properties of these ligands. In order to extend this study to palladium(0) compounds, the polyaromatic phosphines PPh_2Np, PPh_2An, $PPhNp_2$ and PNp_3 (Fig. 1) were reacted with $[Pd_2(dba)_3]{\cdot}CHCl_3$.

When a dichloromethane solution containing four equivalents of PPh_2Np was added to a dichloromethane solution of $[Pd_2(dba)_3]{\cdot}CHCl_3$, a rapid colour change to dark orange occurred. After 4 h some of the solvent was removed under reduced pressure and ether added. The mixture was kept at 4°C and after a few hours orange crystals separated. The product obtained was formulated as $[Pd(dba)(PPh_2Np)_2]$ (**1**) on the basis of $^{31}P\text{-}\{^1H\}$-NMR, IR, FAB-MS and elemental analyses. The presence of the dba was confirmed from the $\nu(CO)$ stretching mode in the IR at 1644 cm^{-1}. In the $^{31}P\text{-}\{^1H\}$-NMR two doublets in a 1:1 ratio were observed at 17.6 and 22.2 ppm. This suggested the presence of two coupled but inequivalent phosphines in the complex. Similar spectroscopic properties have been observed by Herrmann and co-workers for the compound $[Pd(dba)(PCy_3)_2]$ [5]. The inequivalent phosphine environments are a direct consequence of the in-plane coordination of the dba ligand in the resulting trigonal complex and restricted rotation about the Pd-alkene bond:

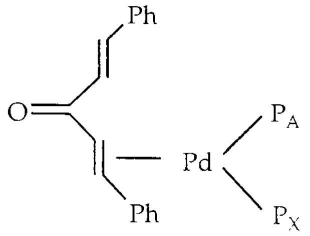

The formulation of the complex as $[Pd(dba)(PPh_2Np)_2]$ was confirmed by a single crystal X-ray crystallographic study. The molecular structure of this complex is shown in Fig. 2 and selected bond lengths and angles are summarised in Table 1.

The palladium atom is three coordinate with a trigonal planar geometry, two of the donors being the phosphorus atoms (mean Pd–P 2.348 Å), and the third site is occupied by one η-olefin of the dba ligand (mean Pd–C 2.22 Å) the second olefin group remaining uncoordinated. The closest approach to the metal centre at the axial position is from a naphthalene hydrogen atom (Pd(1)···H(47) 2.87 Å) suggesting a weak metal-hydrogen agostic interaction.

Similar reactions were carried out using the phosphines PPh_2An and $PPhNp_2$. After 4 h, in both cases, orange products were isolated. These were formulated as $[Pd(dba)(PPh_2An)_2]$ (**2**) and $[Pd(dba)(PPhNp_2)_2]$ (**3**) on the basis of $^{31}P\text{-}\{^1H\}$-NMR, IR, FAB-MS and elemental analyses. The $^{31}P\text{-}\{^1H\}$-NMR spectra of both products showed the same pattern observed for $[Pd(dba)(PPh_2Np)_2]$: two doublets in a 1:1 ratio. The

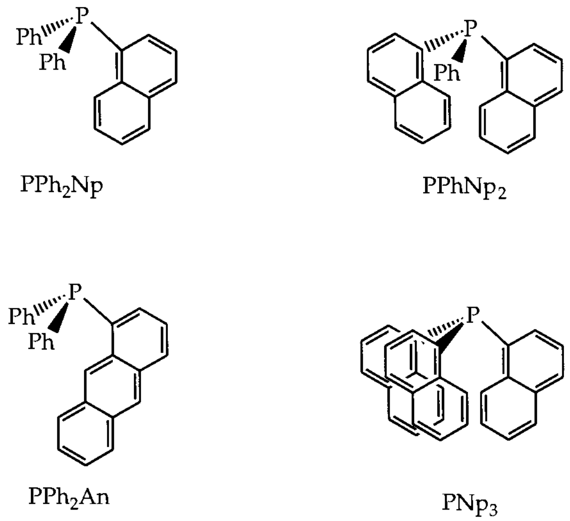

PPh_2Np $PPhNp_2$

PPh_2An PNp_3

Fig. 1. Polyaromatic phosphines used in this work.

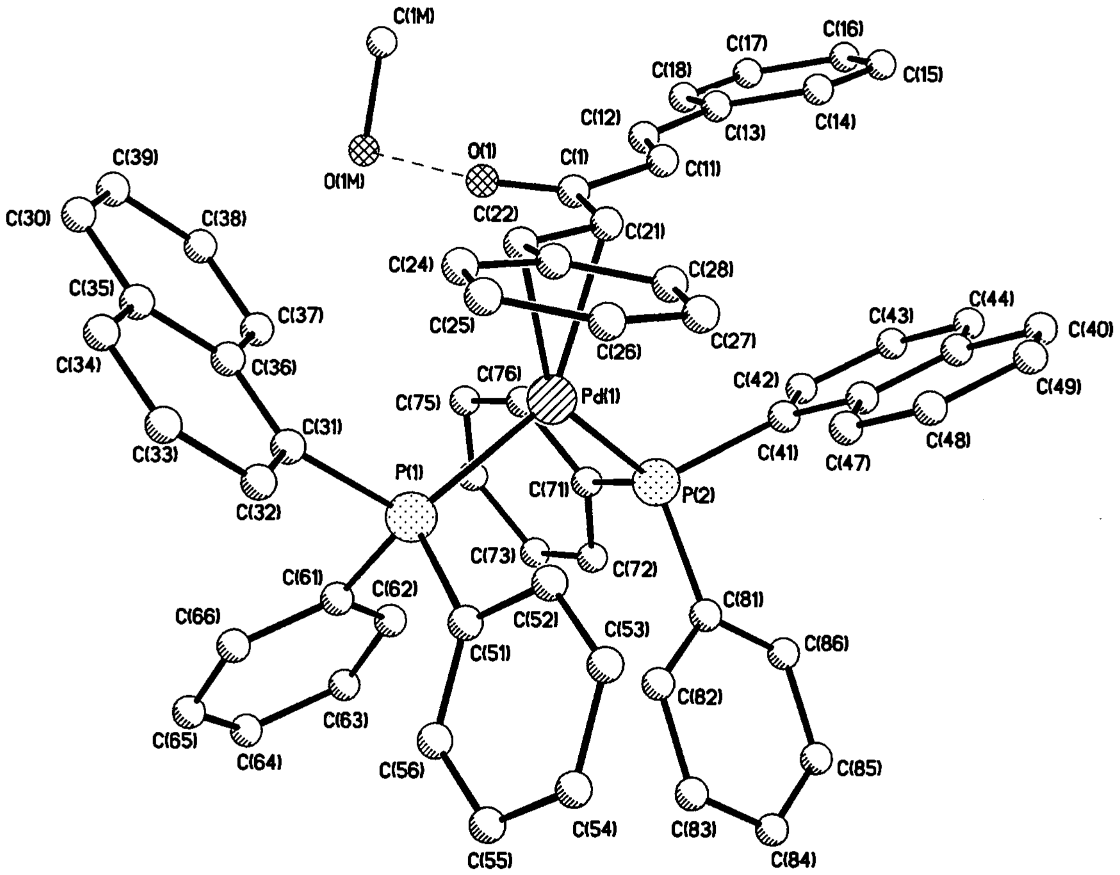

Fig. 2. Molecular structure of **1**.

chemical shifts and coupling constants for these three compounds are summarised in Table 2. The IR spectra of these complexes showed strong bands in the ketonic CO region revealing the presence of dba (Table 2).

The three complexes showed similar FAB mass spectral fragmentation patterns. The highest intensity peak in each case was assigned to the fragment $[Pd(PR_3)_2]$ indicating that under FAB conditions, the dba is rapidly lost from the complex. In Table 3 the major peak assignments for $[Pd(dba)(PNpPh_2)_2]$ are given. Interestingly, for all three complexes, higher molecular weight peaks were observed in the FAB mass spectra than for M^+. These were assigned to the aggregation products $[Pd_2L_2]$ and $[Pd_2L_3]$ (where L = polyaromatic phosphine).

From the results discussed above, the general reaction between $[Pd_2(dba)_3]$ and the polyaromatic phosphines can be summarised as follows:

$$[Pd_2(dba)_3] + 4L \rightarrow 2[Pd(dba)L_2] + dba$$

$$L = PPh_2Np, PPh_2An, PPhNp_2$$

An analogous reaction was carried out using the more sterically demanding phosphine PNp_3. However, even after 24 h no complex formation was observed in the ^{31}P-$\{^1H\}$-NMR. Even on reflux the ^{31}P-$\{^1H\}$-NMR spectrum showed only a singlet at -32.5 ppm that corresponded to the PNp_3. Presumably, the large steric demands of this phosphine prevents it from coordinating to the palladium.

Similar results have been obtained previously for analogous reactions with platinum compounds [11]. For the reaction between $[PtCl_2(COD)]$ or $[Pt(CH_3CN)_4](BF_4)_2$ with the polyaromatic phosphines the following reactivity trend is observed: $PPh_2Np > PPh_2An > PPhNp_2 > PNp_3$. In the case of the reaction between these phosphines and $[Pd_2(dba)_3]$ no large difference in reactivity was observed for PPh_2Np, PPh_2An and $PPhNp_2$. However, the lack of reactivity of PNp_3 suggests that steric factors probably prevent its coordination. The Tolman cone angles for these phosphines have been previously calculated and reported [12]. The calculated cone angles of the polyaromatic phosphines are much larger than that for PPh_3 and increase in the order: $PPh_2An < PPh_2Np < PPhNp_2 < PNp_3$.

It has been previously observed that, in some cases, if an excess of phosphine is added to the $[Pd(dba)L_2]$ compound, dba is displaced giving the complexes $[PdL_3]$ or $[PdL_4]$ [1]. In order to study this possibility for the polyaromatic phosphines, an excess of the phosphine was added to a solution of the compound $[Pd(dba)L_2]$ in toluene. On monitoring the reaction by

Table 1
Selected bond lengths (Å) and angles (°) for **1**

Bond lengths (Å)			
Pd(1)–P(1)	2.338(6)	Pd(1)–P(2)	2.357(6)
Pd(1)–C(21)	2.23(2)	Pd(1)–C(22)	2.21(2)
P(1)–C(31)	1.873(12)	P(1)–C(51)	1.835(12)
P(1)–C(61)	1.815(12)	P(2)–C(41)	1.861(11)
P(2)–C(71)	1.805(12)	P(2)–C(81)	1.812(12)
C(1)–O(1)	1.22(2)	C(1)–C(21)	1.45(3)
C(1)–C(11)	1.51(3)	C(11)–C(12)	1.32(3)
C(12)–C(13)	1.48(3)	C(21)–C(22)	1.44(3)
C(22)–C(23)	1.50(2)		
Bond angles (°)			
P(1)–Pd(1)–P(2)	112.6(2)	C(21)–Pd(1)–C(22)	37.7(7)
C(21)–Pd(1)–P(1)	138.2(6)	C(22)–Pd(1)–P(1)	100.7(6)
C(21)–Pd(1)–P(2)	109.1(6)	C(22)–Pd(1)–P(2)	146.7(6)
C(31)–P(1)–Pd(1)	115.4(4)	C(51)–P(1)–Pd(1)	111.6(5)
C(61)–P(1)–Pd(1)	119.8(6)	C(41)–P(2)–Pd(1)	114.3(4)
C(71)–P(2)–Pd(1)	110.7(5)	C(81)–P(2)–Pd(1)	120.5(6)
C(22)–C(21)–Pd(1)	70.3(12)	C(1)–C(21)–Pd(1)	98.0(12)
C(21)–C(22)–Pd(1)	72.0(11)	C(23)–C(22)–Pd(1)	109.2(12)
O(1)–C(1)–C(21)	126.0(2)	O(1)–C(1)–C(11)	119.0(2)
C(12)–C(11)–C(13)	128.0(2)	C(21)–C(1)–C(11)	115.0(2)
C(22)–C(21)–C(1)	119.0(2)		

$^{31}P\{^1H\}$-NMR during a period of 24 h no change in the spectrum was observed, indicating that in these cases dba is not displaced from [Pd(dba)L_2] by excess L.

2.2. Reaction of [$Pd_2(dba)_3$] with PBz_3

When PBz_3 was reacted with [$Pd_2(dba)_3$]·C_6H_6 in CH_2Cl_2 at r.t. for 4 h, an orange product characterised as [Pd(dba)$(PBz_3)_2$] **4**, was obtained. The formulation of this complex was confirmed by an X-ray structural characterisation (Fig. 3, Table 4). Crystals of **4** were grown by layering a toluene solution with methanol.

Table 2
^{31}P-$\{^1H\}$-NMR data for the compounds [Pd(dba)L_2] (L = PPh_2Np, PPh_2An, $PPhNp_2$ and PBz_3)

L	δ (ppm)	$^2J(P_{ab})$ (Hz)	νCO (cm^{-1})
PPh_2Np	22.2 (d) 17.6 (d)	9.4	1644
PPh_2An	7.9 (d) 2.0 (d)	17.0	1647
$PPhNp_2$	28.5 (d) 26.1 (d)	23.8	1644
PBz_3	8.1 (d) 7.6 (d)	8.4	1643

Table 3
Details for the positive ion FAB mass spectrum of M = [Pd(dba)$(PPh_2Np)_2$]

m/z	Intensity (%)	Fragment
730	100	$[M\text{-dba}]^+$
418	10	$[M\text{-dba-}PPh_2Np]^+$
341	5	$[M\text{-dba-}PPh_2Np\text{-Ph}]^+$
214	5	$[M\text{-dba-}PPh_2Np\text{-Ph-Np}]^+$

There are two independent molecules in the unit cell which are almost identical and both have planar three coordinate geometries if the centre of the olefinic bond is defined as a coordination site. The structure resembles that observed for **1** with bond lengths to the palladium atom being slightly shorter (mean Pd–P 2.325 Å, mean Pd–C 2.19 Å), though the differences are on the edge of being statistically significant. In both **1** and **4** the phosphorus and the olefin atoms are nearly coplanar with the metal (maximum deviation −0.058 Å for C(21) in **1**, and 0.097 and 0.068 Å for C(12) and C(32), respectively in the two molecules of **4**). The closest approaches to the metal centres in **4** at the axial positions are from the phenyl hydrogen atoms (Pd(1)···H(13a) 2.83 Å, Pd(2)···H(43a) 2.72 Å). In the crystals of both **1** and **4**, methanol molecules have been found to be hydrogen bonded to the ketone oxygen atoms of the dba ligands (O(1m)···O(1) 2.769 Å in **1** and O(1m)···O(1) 2.921 Å).

Even though in the solid state **4** has a trigonal planar structure (analogous to that described for the polyaromatic phosphine complexes) in solution its behaviour is more complex. The ^{31}P-$\{^1H\}$-NMR spectrum of **4** in CH_2Cl_2 shows the expected AX pattern (like the NMR spectra of **1**–**3**). However, in toluene or benzene at r.t., the ^{31}P-$\{^1H\}$-NMR spectrum of this compound consists of a broad singlet at around 9.4 and two small and broad signals at 11.0 and 8.2 ppm, which is inconsistent with the proposed formulation. A variable temperature ^{31}P-$\{^1H\}$-NMR study was carried out but it did not yield any further information concerning the solution structure. A complex process seems to be occurring in solution. We believe that, besides a fluxional process involving the coordinated phosphines, there may be an equilibrium which involves the formation of dimeric species such as [$Pd_2(\mu\text{-dba})_2(PBz_3)_2$]. We are currently exploring this and other species that might be responsible for the unexpected behaviour of this system in solution.

2.3. Reaction between [$Pd_2(dba)_3$] and PBz_3 in the presence of SO_2

The reactions between [$Pd_2(dba)_3$]·$CHCl_3$ and PR_3 in the presence of SO_2 have been previously reported for a wide range of phosphines. The majority of the phosphines studied give the pentanuclear clusters [$Pd_5(\mu_3\text{-}SO_2)_2(\mu\text{-}SO_2)_2(L)_5$] where L = PPh_3, $PMePh_2$, PMe_2Ph, $P(C_6H_4OMe\text{-}p)_3$, $P(C_6H_4OMe\text{-}m)_3$, or $AsPh_3$ [8]. When L = PMe_3, the tetranuclear cluster [$Pd_4(SO_2)_3(PMe_3)_5$], which is based on a butterfly structure, is obtained. PCy_3, which has a larger Tolman cone angle, gives [$Pd_4(SO_2)_3(PCy_3)_4$], which has a tetrahedral metal cluster geometry [8].

A SO_2-saturated toluene solution of PBz_3 was added to a toluene solution of [$Pd_2(dba)_3$]·C_6H_6 and SO_2 was

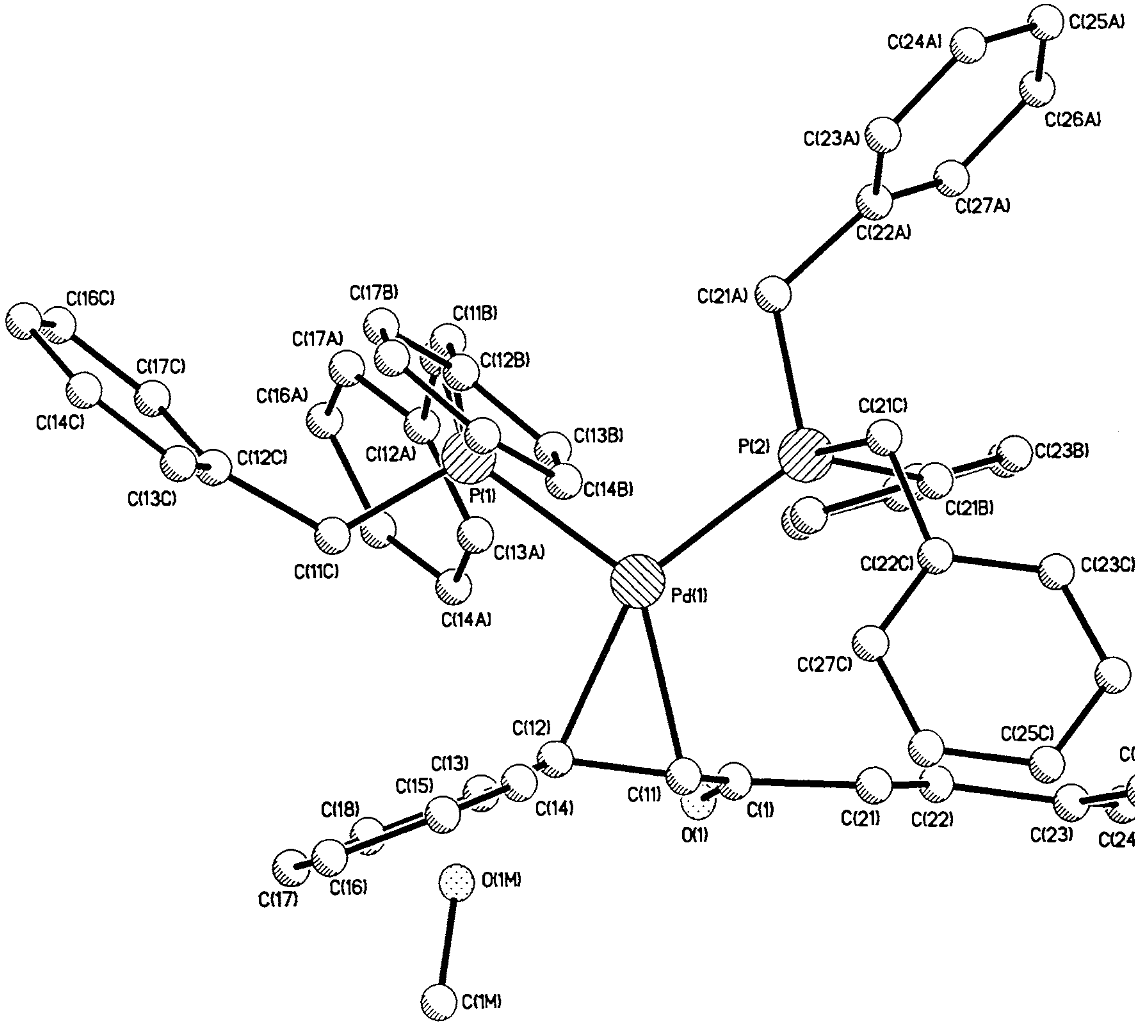

Fig. 3. Molecular structure of **4**.

bubbled through the solution for an additional 10 min leading to a change in colour to dark red. After removal of the solvent under reduced pressure, followed by washing with several portions of ethanol to remove the free dba, and recrystallisation from toluene/diethyl ether, yellow crystals were obtained. A $(CD_3)_2CO$ solution of the crystals gave rise to a sharp singlet in the $^{31}P\{^1H\}$-NMR spectrum with a chemical shift of 2.8 ppm relative to H_3PO_4, indicating that all the phosphorus atoms in the product are chemically equivalent.

In general the reaction of $[Pd_2(dba)_3]$ with a phosphine under an atmosphere of sulfur dioxide gas results in the formation of SO_2-containing cluster compounds which do not contain any dba coordinated to the metals. However, in this reaction, the product, after several washings with ethanol followed by recrystallisation, contained a peak at 1606 cm^{-1} in the IR spectrum, that corresponds to the carbonyl stretching vibration in the dba ligand. Peaks at 1195 and 1054 cm^{-1} in the IR spectrum confirmed the presence of sulfur dioxide. A high carbon content (63%) was found in the microanalysis of the compound, also indicating that the dba ligand was present in the product of this reaction. On the basis of the spectroscopic and analytical data alone it was not possible to propose an unambiguous structure for this compound. Fortunately, crystals of sufficiently good quality were obtained so that a single crystal X-ray analysis could be carried out. The molecular structure of **5** is shown in Fig. 4; selected bond lengths and angles are given in Table 5.

The molecular structure of **5** consists of a palladium dimer with the palladium atoms bridged by one SO_2 and one dba ligand; each palladium atom is also bonded to one tribenzylphosphine ligand. The triangular coordination geometry observed in **1** and **4** is slightly distorted in **5** by the presence of the Pd–Pd interaction (2.885(2) Å). Similar Pd–Pd bond lengths have been reported in related SO_2-bridged palladium clusters, and range from 2.7720(7) to 2.956(5) Å [8]. In **5** the bridging mode adopted by the dba ligand results from the coordination of the two olefin groups to the two palladium atoms. The conformation of the dba in

5 is clearly *cis*, *cis* while in the dimeric structure $[Pd_2(dba)_3]·CHCl_3$ the dba adopts a different conformation: *cis*, *trans*.

It is interesting to note that the labile dba ligand remains in the dimer, without aggregation of the '$[Pd_2(SO_2)(PBz_3)_2]$' fragment into a higher nuclearity cluster. The recent work of Amatore and co-workers has established that the dba ligand is indeed not as labile as was previously thought [13]. These findings are consistent with the reactivity when $L = PBz_3$ in the system $[Pd_2(dba)_3] + SO_2 + L$. The $[Pd_5(SO_2)_4(L)_5]$ structure is adopted by a large range of phosphines with differing sizes and electronic properties, from PMe_3 with a cone angle of 118° to PPh_3 with a cone angle of 145°. In the case of the analogous reaction with PCy_3 (cone angle 170°), the tetranuclear cluster $[Pd_4(SO_2)_3(PCy_3)_4]$ is obtained. However PBz_3, with its smaller cone angle of 165° gives only a Pd_2 species and retains a dba ligand. Clearly the formation of particular cluster sizes does not depend only on the ligand cone angle and must represent a subtle compromise between steric and electronic effects. In this system, PBz_3 shows anomalous behaviour as a result of these factors, affording a novel Pd(0) dimer which may act as a convenient source for the '$[Pd_2(SO_2)(PBz_3)_2]$' fragment. We are currently studying the reactivity of this dimer and some preliminary results are summarised in Scheme 1. This will be reported in full at a later time.

Table 4
Selected bond lengths (Å) and angles (°) for **4**

Bond lengths (Å)			
Pd(1)–P(1)	2.313(8)	Pd(2)–P(3)	2.364(9)
Pd(1)–P(2)	2.343(8)	Pd(2)–P(4)	2.328(9)
Pd(1)–C(11)	2.22(2)	Pd(2)–C(31)	2.10(3)
Pd(1)–C(12)	2.18(3)	Pd(2)–C(32)	2.25(3)
P(1)–C(11a)	1.86(3)	P(2)–C(21a)	1.86(3)
P(1)–C(11b)	1.79(3)	P(2)–C(21b)	1.85(3)
P(1)–C(11c)	1.78(3)	P(2)–C(21c)	1.93(3)
P(3)–C(31a)	1.85(3)	P(4)–C(41a)	1.87(3)
P(3)–C(31b)	1.81(3)	P(4)–C(41b)	1.93(3)
P(3)–C(31c)	1.83(3)	P(4)–C(41c)	1.81(3)
O(1)–C(1)	1.32(4)	O(2)–C(2)	1.29(3)
C(1)–C(11)	1.27(5)	C(2)–C(41)	1.42(4)
C(1)–C(21)	1.55(4)	C(2)–C(31)	1.61(4)
C(11)–C(12)	1.45(4)	C(31)–C(32)	1.38(4)
C(12)–C(13)	1.35(4)	C(32)–C(33)	1.56(3)
C(21)–C(22)	1.32(4)	C(41)–C(42)	1.31(5)
C(22)–C(23)	1.55(3)	C(42)–C(43)	1.41(3)
Bond angles (°)			
P(1)–Pd(1)–P(2)	107.2(3)	P(3)–Pd(2)–P(4)	107.2(3)
C(11)–Pd(1)–C(12)	38.6(9)	C(31)–Pd(2)–C(32)	36.8(11)
C(11)–Pd(1)–P(1)	139.6(7)	C(31)–Pd(2)–P(4)	136.3(9)
C(12)–Pd(1)–P(1)	101.2(7)	C(32)–Pd(2)–P(4)	99.8(8)
C(11)–Pd(1)–P(2)	113.2(7)	C(31)–Pd(2)–P(3)	116.4(9)
C(12)–Pd(1)–P(2)	151.0(7)	C(32)–Pd(2)–P(3)	152.9(7)
C(1)–C(11)–Pd(1)	98.0(2)	C(2)–C(31)–Pd(2)	102.0(2)
C(12)–C(11)–Pd(1)	69.4(14)	C(31)–C(32)–Pd(2)	66.0(2)
C(11)–C(12)–Pd(1)	72.0(2)	C(32)–C(31)–Pd(2)	77.0(2)
C(13)–C(12)–Pd(1)	125.0(2)	C(33)–C(32)–Pd(2)	112.0(2)
O(1)–C(1)–C(11)	135.0(3)	O(2)–C(2)–C(41)	122.0(3)
O(1)–C(1)–C(21)	108.0(3)	O(2)–C(2)–C(31)	115.0(2)
C(11)–C(1)–C(21)	116.0(3)	C(41)–C(2)–C(31)	123.0(2)
C(1)–C(11)–C(12)	125.0(3)	C(32)–C(31)–C(2)	116.0(2)
C(1)–C(21)–C(22)	121.0(3)	C(42)–C(41)–C(2)	130.0(3)
C(11)–C(12)–C(13)	132.0(3)	C(31)–C(32)–C(33)	116.0(2)
C(21)–C(22)–C(23)	128.0(2)	C(41)–C(42)–C(43)	128.0(3)

3. Conclusion

The reactions between $[Pd_2(dba)_3]$ and series of sterically demanding phosphines have been studied. The products obtained have been formulated as $[Pd(dba)L_2]$ (where $L = PPh_2An$, PPh_2Np, $PPhNp_2$ and PBz_3) and single crystal X-ray structural analyses of $[Pd(dba)(PPh_2Np)_2]$ and $[Pd(dba)(PBz_3)_2]$ have confirmed that these complexes adopt a trigonal planar structure with the dba ligand coordinated by a simple double bond. The $^{31}P\{^1H\}$-NMR spectra of these compounds in CH_2Cl_2 solutions show a clear AX pattern. However, this is not the case when the $^{31}P\{^1H\}$-NMR spectrum of $[Pd(dba)(PBz_3)_2]$ is studied in benzene or toluene solution. An equilibrium involving a dimeric species might be responsible for the anomalous behaviour. When the reaction between $[Pd_2(dba)_3]$ and PBz_3 was carried out under an SO_2 atmosphere the novel dimer $[Pd_2(\mu\text{-dba})(\mu\text{-}SO_2)(PBz_3)_2]$ was formed. This formulation has been confirmed by a single crystal X-ray structural analysis.

4. Experimental

4.1. General procedures and instrumentation

All the reactions were routinely carried out using standard Schlenk line techniques under an atmosphere of pure nitrogen. The solvents used were dry and free of oxygen. $[Pd_2(dba)_3] \cdot CHCl_3$ and $[Pd_2(dba)_3] \cdot C_6H_6$ were synthesised according to previously reported methods [1]. IR spectra were recorded in a Perkin-Elmer 1720 IR Fourier transform spectrometer between 4000 and 250 cm^{-1} as KBr pellets. $^{31}P\text{-}\{^1H\}$-NMR spectra were recorded on a JEOL JNM-EX270 Fourier transform NMR spectrometer operating at a frequency of 290 MHz with chemical shifts reported relative to TMS and H_3PO_4, respectively. Mass spectra were recorded by J. Barton at Imperial College on a VG AutoSpec-Q as FAB using 3-NBA as matrix. Microanalyses (C, H, N) were carried out by H. O'Callaghan at Imperial College.

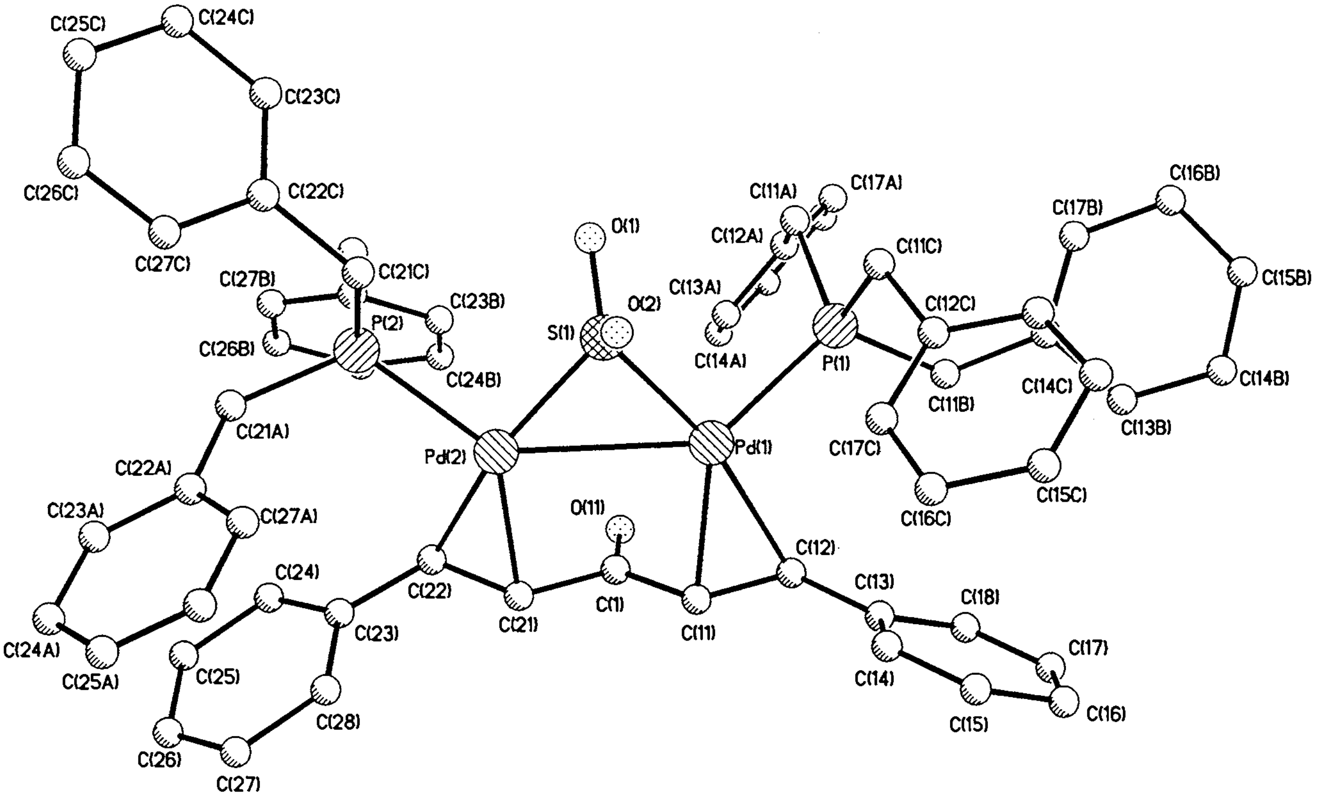

Fig. 4. Molecular structure of **5**.

4.2. Preparations

4.2.1. [Pd(dba)(PPh$_2$Np)$_2$] 1

[Pd$_2$(dba)$_3$]·CHCl$_3$ (0.11 g, 0.1 mmol) was dissolved in toluene (20 ml) and a solution of PPh$_2$Np (0.13 g, 0.4 mmol) in toluene (20 ml) added. The reaction mixture was stirred at r.t. for 4 h. The solvent was removed under reduced pressure and a dark brown solid was obtained. This solid was washed with ether giving an orange solution from which [Pd(dba)(PPh$_2$Np)$_2$] was obtained as a pure yellow-orange solid by addition of hexane (0.099 g, 51%). Anal. Calc.: found C 75.9%, H 5.0%; C$_{61}$H$_{44}$OP$_2$Pd requires: C 75.9%, H 5.0%. ^{31}P-{^{1}H}-NMR: Solution (d$_8$-toluene) δ at 22.2 ppm (1P, d) and 17.6 ppm (1P,d), ^2J(P$_a$P$_b$) = 9.4 Hz. IR ν(CO) 1644 cm^{-1}. FAB mass spectrum: see text.

4.2.2. [Pd(dba)(PPh$_2$An)$_2$] 2

This compound was synthesised by the same method as for [Pd(dba)(PPh$_2$Np)$_2$] using: [Pd$_2$(dba)$_3$]·CHCl$_3$ (0.10 g, 0.1 mmol) and PPh$_2$An (0.15 g, 0.4 mmol). The reaction mixture was stirred at r.t. for 4 h. The solvent was removed under reduced pressure and a dark brown solid was obtained. This solid was washed with ether obtaining an orange solution from which [Pd(dba)(PPh$_2$An)$_2$] crystallised as an orange solid (0.08 g, 37%). Anal. Calc.: C 75.8%, H 4.6%; required for C$_{69}$H$_{52}$OP$_2$Pd C 77.8%, H 4.9%. ^{31}P-{^{1}H}-NMR: Solution (d$_8$-toluene) δ at 7.9 ppm (1P, d) and 2.0 ppm (1P,d), ^2J(P$_a$P$_b$) = 17 Hz. IR ν(CO) 1647 cm^{-1}.

4.2.3. [Pd(dba)(PPhNp$_2$)$_2$] 3

The same method as for [Pd(dba)(PPh$_2$Np)$_2$] was carried out using: [Pd$_2$(dba)$_3$]·CHCl$_3$ (0.10 g, 0.1 mmol) and PPhNp$_2$ (0.15 g, 0.4 mmol). [Pd(dba)(PPh$_2$Np)$_2$] was obtained as a pure yellow-orange solid that precipitated with the addition of hexane to the ether solution (0.09 g, 42.2%) Anal. Calc.: C 77.6%, H, 4.6%. C$_{69}$H$_{52}$OP$_2$Pd requires C 77.8%, H 4.9%. ^{31}P-{^{1}H}-NMR: Solution (d$_8$-toluene) δ at 28.5 ppm (1P, d) and 26.1 ppm (1P,d), ^2J(P$_a$P$_b$) = 23.8 Hz. IR ν(CO) 1644 cm^{-1}.

4.2.4. [Pd(dba)(PBz$_3$)$_2$] 4

The same method as for [Pd(dba)(PPh$_2$Np)$_2$] was carried out using: [Pd$_2$(dba)$_3$]·C$_6$H$_6$ (0.20 g, 0.2 mmol) and PBz$_3$ (0.25 g, 0.81 mmol). The reaction mixture was stirred at r.t. for 4 h. After filtration the orange solution was reduced to 5 ml followed by the addition of a layer of MeOH. The mixture was kept at 4°C for 2 days. Orange crystals of [Pd(dba)(PBz$_3$)$_2$] were obtained (0.12 g, 61%). Some of these crystals were suitable for an X-ray analysis. Anal. Calc.: C 73.1%, H 5.6%. C$_{59}$H$_{57}$OP$_2$Pd·CH$_3$OH requires C 73.4%, H 6.1%. ^{31}P-{^{1}H}-NMR: Solution (CD$_2$Cl$_2$) δ at 8.1 ppm (1P, d) and 7.6 ppm (1P,d), ^2J(P$_a$P$_b$) = 8.4. Hz. IR ν(CO) 1643 cm^{-1}. FAB-MS$^+$: $m/v = 949$ {[M]$^+$}, 822 {[Pd$_2$(PBz$_3$)$_2$]$^+$}, 731 {[Pd$_2$(PBz$_3$)(PBz$_2$)]$^+$}.

4.2.5. [Pd$_2$(μ-dba)(μ-SO$_2$)(PBz$_3$)$_2$] **5**

PBz$_3$ (184 mg, 0.60 mmol) was dissolved in toluene (15 ml) and SO$_2$ gas was bubbled through for 1 min. This solution was then added to a solution of [Pd$_2$(dba)$_3$]·C$_6$H$_6$ (300 mg, 0.30 mmol) in toluene (25 ml), and SO$_2$ gas bubbled through the solution for 10 min whereupon the colour of the solution had changed from deep purple to red. The mixture was stirred under an atmosphere of SO$_2$ for a further 30 min to ensure completion of the reaction. The solvent was removed under reduced pressure and the yellow-red residue was washed with two successive 30 ml portions of ethanol to remove the free dba. The remaining yellow powder was recrystallized from a toluene/diethyl ether mixture and cooled slowly to 4°C (0.302 g, 89%). Some of these crystals were suitable for a single-crystal X-ray analysis. Anal. Calc.: C, 63.0%; H, 5.3% (C$_{59}$H$_{56}$O$_3$P$_2$Pd$_2$S requires: C, 63.2%; H, 5.0%). ν_{max}/cm^{-1} 1606 (C=O), 1195 (SO$_2$), 1054 (SO$_2$). δ_P ((CD$_3$)$_2$CO) 2.8 (s). FAB-MS$^+$: $m/v =$ 1120 {[M]$^+$}, 822 {[Pd$_2$(PBz$_3$)$_2$]$^+$}, 731 {[Pd$_2$(PBz$_3$)(PBz$_2$)]$^+$}.

Table 5
Selected bond lengths (Å) and angles (°) for **5**

Bond lengths (Å)			
Pd(1)–Pd(2)	2.885(2)		
Pd(1)–P(1)	2.325(4)	Pd(2)–P(2)	2.335(4)
Pd(1)–C(11)	2.232(13)	Pd(2)–C(21)	2.242(12)
Pd(1)–C(12)	2.334(13)	Pd(2)–C(22)	2.35(2)
Pd(1)–S(1)	2.246(4)	Pd(2)–S(1)	2.252(4)
S(1)–O(2)	1.458(11)	S(1)–O(1)	1.473(10)
P(1)–C(11A)	1.84(2)	P(2)–C(21A)	1.806(14)
P(1)–C(11B)	1.856(14)	P(2)–C(21B)	1.838(14)
P(1)–C(11C)	1.82(2)	P(2)–C(21C)	1.874(14)
C(1)–O(11)	1.26(2)	C(1)–C(11)	1.42(2)
C(1)–C(21)	1.49(2)	C(11)–C(12)	1.41(2)
C(12)–C(13)	1.49(2)	C(13)–C(14)	1.38(2)
C(13)–C(18)	1.43(2)	C(14)–C(15)	1.36(2)
C(15)–C(16)	1.39(2)	C(16)–C(17)	1.45(2)
C(17)–C(18)	1.35(2)	C(21)–C(22)	1.40(2)
C(22)–C(23)	1.47(2)		
Bond angles (°)			
Pd(1)–S(1)–Pd(2)	79.80(12)	O(2)–S(1)–O(1)	113.9(6)
O(2)–S(1)–Pd(1)	112.7(5)	O(1)–S(1)–Pd(1)	116.9(4)
O(2)–S(1)–Pd(2)	117.4(4)	O(1)–S(1)–Pd(2)	112.1(5)
P(1)–Pd(1)–Pd(2)	139.10(11)	P(2)–Pd(2)–Pd(1)	140.25(11)
S(1)–Pd(1)–Pd(2)	50.19(10)	S(1)–Pd(2)–Pd(1)	50.01(9)
C(11)–Pd(1)–Pd(2)	84.0(3)	C(21)–Pd(2)–Pd(1)	83.7(4)
C(12)–Pd(1)–Pd(2)	118.9(4)	C(22)–Pd(2)–Pd(1)	113.4(3)
C(11)–Pd(1)–S(1)	132.2(3)	C(21)–Pd(2)–S(1)	133.5(4)
S(1)–Pd(1)–P(1)	93.64(14)	S(1)–Pd(2)–P(2)	91.21(14)
S(1)–Pd(1)–C(12)	168.0(4)	S(1)–Pd(2)–C(22)	159.4(4)
C(11)–Pd(1)–P(1)	134.1(3)	C(21)–Pd(2)–P(2)	135.3(4)
P(1)–Pd(1)–C(12)	98.3(3)	P(2)–Pd(2)–C(22)	101.8(4)
C(11)–Pd(1)–C(12)	35.9(5)	C(21)–Pd(2)–C(22)	35.4(5)
C(12)–C(11)–Pd(1)	76.0(8)	C(22)–C(21)–Pd(2)	76.6(8)
C(1)–C(11)–Pd(1)	89.8(9)	C(1)–C(21)–Pd(2)	96.1(8)
C(11)–C(12)–Pd(1)	68.1(7)	C(21)–C(22)–Pd(2)	67.9(8)
C(23)–C(22)–Pd(2)	121.9(10)	C(13)–C(12)–Pd(1)	115.1(9)
C(11)–C(1)–C(21)	113.6(14)	O(11)–C(1)–C(21)	121(2)
O(11)–C(1)–C(11)	125.6(14)	C(22)–C(21)–C(1)	125(2)
C(12)–C(11)–C(1)	123.0(14)	C(21)–C(22)–C(23)	121.7(14)
C(11)–C(12)–C(13)	121.8(14)		

4.3. Crystallography

X-ray intensity data for compounds **1**, **4** and **5** were collected on a Siemens P4 diffractometer equipped with a Siemens LT2 low temperature device, using graphite Mo–K$_\alpha$ radiation and a $\omega - 2\theta$ scan. The crystal data, data collection and refinement are summarised in Table 6. In all cases, three standard reflections measured after every 97 reflections showed no significant variation in intensity throughout data collection. The data were corrected for Lorentz and polarisation factors and absorption effects.

4.3.1. Structure solution and refinement [14]

The structures of compounds **1**, **4** and **5** were solved by direct methods which revealed nearly all the non-hydrogen atoms and, in each case, the remaining non-hydrogen atoms were located from subsequent difference-Fourier syntheses. In the asymmetric unit of **4**, two molecular units were observed. In **1** and **5**, all the phenyl rings were constrained to refine as regular hexagons. In both cases, the phenyl hydrogen atoms were placed in idealised position with displacement parameters equal to 1.2 U_{eq} of the parent carbon atom of the phenyl groups. In **4**, the methylene hydrogen atoms were also placed in idealised geometry but their assigned displacement parameters were equal to 1.5 U_{eq} of the parent carbon atom. For all three compounds **1**, **4** and **5**, empirical absorption corrections were applied to the data after initial refinement with isotropic displacement parameters for all atoms [15]. In **1**, a total of 12 residual peaks, each ca. 1 e Å^{-3}, in a planar disposition, were assigned as a severely disordered benzene ring, one of the solvent molecules used in the reaction, this disorder accounts for the poor diffraction by the crystal. In all cases, all non-hydrogen atoms were assigned anisotropic displacement parameters in the final cycles of full-matrix least-squares refinement, based on F^2.

Acknowledgements

We thank EPSRC for financial support and BP plc for endowing D.M.P.M.'s chair.

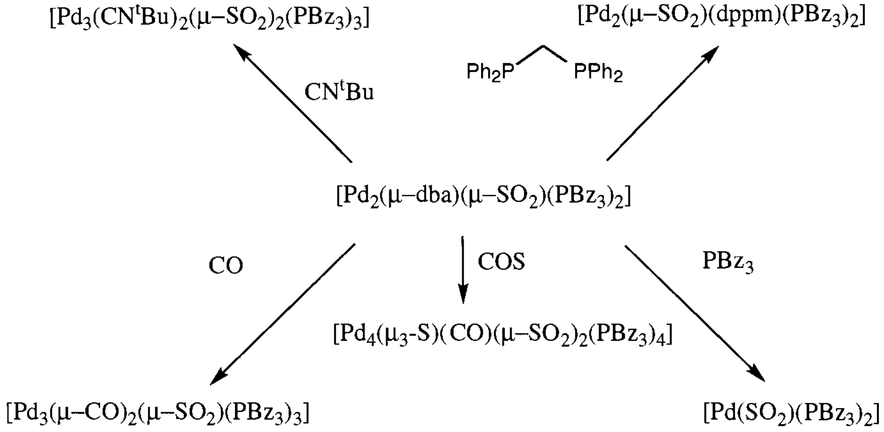

Scheme 1. Preliminary results on the reactivity of **5**.

Table 6
Crystal data and structure refinement for **1**, **4** and **5**

	1	**4**	**5**
Empirical formula	$C_{68}H_{56}O_2P_2Pd$	$C_{60}H_{60}O_2P_2Pd$	$C_{59}H_{56}O_3P_2Pd_2S$
Formula weight	1073.47	1962. 84	1119.84
Temperature (K)	223(2)	223(2)	293(2)
Crystal system	Monoclinic	Monoclinic	Monoclinic
Space group	$P2_1/c$	Cc	$C2/c$
Unit cell dimension			
a (Å)	9.704(3)	20.115(4)	40.256(8)
b (Å)	24.360(6)	11.652(2)	16.992(3)
c (Å)	23.978(9)	42.481(6)	14.896(3)
β (°)	94.19(4)	92.080(12)	98.86(3)
V (Å^3)	5653(3)	9950(3)	10068(4)
Z	4	8	8
D_{calc} (g cm^{-3})	1.261	1.310	1.478
μ(Mo–K_α) (mm^{-1})	0.429	0.480	0.865
F(000)	2224	4096	4576
Crystal size (mm^{-1})	$0.20\times0.38\times0.40$	$0.30\times0.38\times0.40$	$0.04\times0.35\times0.46$
θ-range (°)	1.19–19	2.02–25.00	1.30–25.00
Limiting hkl	−1 to 11, −1 to 28, −28 to 28	−1 to 23, −1 to 13, −50 to 50	−47 to 47, 0 to 20, 0 to 17
Reflections collected	12 796	10 594	10 295
Independent reflections	4538 [$R_{int}=0.1457$]	9550 [$R_{int}=0.1227$]	8848 [$R_{int}=0.1130$]
Data/restraints/parameters	3719/132/531	9525/44/979	8847/0/604
S on F^2	1.077	1.023	1.016
Final R indices[$I>2\sigma(I)$]	$R_1=0.0997$, $wR_2=0.2062$	$R_1=0.0884$, $wR_2=0.2016$	$R_1=0.0932$, $wR_2=0.1757$
R indices (all data)	$R_1=0.2279$, $wR_2=0.2979$	$R_1=0.1477$, $wR_2=0.2601$	$R_1=0.2116$, $wR_2=0.2347$
Largest diff. peak and hole/ e Å^{-3}	0.875 and −0.526	1.488 and −1.093	1.034 and −1.133

Data in common: Mo–K_α ($\lambda=0.71073$); Refinement method full-matrix least-squares on F^2; $S=[\Sigma w(F_o^2-F_c^2)^2/(n-p)]^{1/2}$, where n = number of reflection and p = total number of parameters; $R_1=\Sigma\|F_o|-|F_c\|/\Sigma|F_o|$, $wR_2=\Sigma[w(F_o^2-F_c^2)^2]/\Sigma[w(F_o^2)^2]^{1/2}$, $w^{-1}=[\sigma^2(F_o^2)+({}'P)^2+({}''P)]$ where $P=[\max(F_o^2,0)+2(F_c^2)]/3$ and for **1** $t=0.0987$ and $u=0.00$, for **4** $t=0.0642$ and $u=0.00$ and for **5** $t=0.0584$ and $u=276.623$.

References

[1] T. Ukai, H. Kawazura, Y. Ishii, J.J. Bonnet, J.A. Ibers, J. Organomet. Chem. 65 (1974) 253.

[2] J. Tsuji, Palladium Reagents and Catalysts: Innovations in Organic Synthesis, Wiley, Chichester, 1995.

[3] A.Z. Rubezhov, Russ. Chem. Rev. 57 (1988) 1194.

[4] C. Amatore, A. Jutand, F. Khalil, M.A. M'Barki, L. Mottier, Organometallics 12 (1993) 3168.

[5] W.A. Herrmann, W.R. Thiel, C. Broβmer, K. Öfele, T. Priermeier, S. Scherer, J. Organomet. Chem. 461 (1993) 51.

[6] J. Andrieu, P. Braunstein, A.D. Burrows, J. Chem. Res (S) (1993) 380.

[7] F. Paul, J. Patt, J.F. Hartwig, Organometallics 14 (1995) 3030.

[8] (a) S.G. Bott, O.J. Ezomo, D.M.P. Mingos, J. Chem. Soc. Chem. Commun. (1988) 1048. (b) A.D. Burrows, D.M.P. Mingos, H.R. Powell, J. Chem. Soc. Dalton Trans. (1992) 261. (c) A.D. Burrows, D.M.P. Mingos, Transition Met. Chem. 18 (1993) 129.

[9] (a) A. Christofides, J. Organomet. Chem. 259 (1983) 355. (b) A.D. Burrows, H. Fleischer, D.M.P. Mingos, J. Organomet. Chem. 433 (1992) 311. (c) M. Bochmann, I. Hawkins, M.B. Hursthouse, R.L. Shart, Polyhedron 6 (1987) 1987.

[10] D.M.P. Mingos, T.E. Müller, J. Organomet. Chem. 500 (1995) 251.
[11] T.E. Müller, J.C. Green, S. Menzer, D.M.P. Mingos, M. McPartlin, D.J. Williams, C. Wittingham, T. Woodroffe, J. Organomet. Chem. (in press).
[12] T.E. Müller, PhD Thesis, University of London, 1995.
[13] C. Amatore, A. Jutand, F. Khalil, M. A. M'Barki, L. Mottier, Organometallics 12 (1993) 3168.
[14] SHELXTL (PC version 5.03) Siemens Analytical Instruments Inc., Madison, WI, 1994.
[15] N. Walker, D. Stuart, Acta Crystallogr. 39 (Section A) (1983) 158.